ELSEVIER

Contents lists available at ScienceDirect

# **Environmental Pollution**

journal homepage: www.elsevier.com/locate/envpol





Per- and polyfluorinated alkyl substances (PFAS) in the Scheldt Estuary: Insights from target, suspect and non-target screening of water, sediment and bivalves<sup>\*</sup>

Musa Bonso <sup>a,b,\*</sup>, Francesca Cappelli <sup>c</sup>, Fabian Simon <sup>c</sup>, Katrin Vorkamp <sup>d</sup>, Laetitia Six <sup>e</sup>, Georgios Niarchos <sup>f</sup>, Adrian Covaci <sup>c</sup>, Lieven Bervoets <sup>a</sup>, Thimo Groffen <sup>a</sup>

- <sup>a</sup> ECOSPHERE, Department of Biology, University of Antwerp, Groenenborgerlaan 171, 2020, Antwerp, Belgium
- <sup>b</sup> Department of Environmental Health, Bule Hora University, P.O. Box-144, Bule Hora, Ethiopia
- <sup>c</sup> Toxicological Centre, University of Antwerp, Universiteitsplein 1, 2610, Wilrijk, Belgium
- <sup>d</sup> Department of Environmental Science, Aarhus University, Frederiksborgvej 399, 4000, Roskilde, Denmark
- <sup>e</sup> Public Waste Agency of Flanders (OVAM), Stationsstraat 110, 2800, Mechelen, Belgium
- f Department of Aquatic Sciences and Assessment, Swedish University of Agricultural Sciences, PO Box 7050, SE-750 07, Uppsala, Sweden

#### ABSTRACT

Per- and polyfluoroalkyl substances (PFAS) are a concern due to their persistence and widespread environmental distribution. This study analysed PFAS in water, sediment, and bivalves (resident blue mussels and translocated Asian clams) along the Scheldt Estuary (the Netherlands-Belgium) using target, suspect screening (SS), and non-target analysis (NTA). As a result, various PFAS, including ultra-short-, short-, and long-chain PFAS, were detected in varying concentrations. Targeted analysis detected 8 PFAS in water ( $\sum$ PFAS: 9.4–585 ng/L), 11 PFAS in sediment ( $\sum$ PFAS: 7.5–47.8 ng/g dw), and 8 PFAS in bivalves ( $\sum$ PFAS: 1.8–17.5 ng/g ww). SS and NTA detected 7 to 9 additional PFAS in each matrix, with estimated  $\sum$ PFAS concentrations ranging from 883 to 6421 ng/L in water, 49 to 110 ng/g dw in sediment, and 42 to 111 ng/g ww in bivalves. Short-chain PFAS dominated the relative contributions to  $\sum$ concentrations in each matrix. The Environmental Quality Standard (EQS) for perfluorooctanesulfonate (PFOS) in surface water (0.65 ng/L) was exceeded at most locations, while in bivalves it remained below the biota EQS of 9.1 ng/g ww at all sites. Estimated  $\sum$ PFAS concentrations based on SS and NTA generally exceeded results from targeted analysis in each matrix, emphasizing the importance of untargeted methods for comprehensive PFAS monitoring and risk assessments. Notably, trifluoromethanesulfonic acid (TFMS) dominated at an industrial estuary reach, while several precursors were tentatively annotated. Multivariate analyses indicated inverse correlations between bivalve-sediment  $\sum$ PFAS and positive sediment PFAS correlations with TOC and clay, indicating sorption-limited bioavailability. While this study provides valuable insights on the distribution of PFAS in estuarine ecosystems, future studies should consider suspended particulate matter and tidal cycles to better understand the environmental fate of these contaminants.

## 1. Introduction

Per- and polyfluoroalkyl substances (PFAS), as defined by the Organization for Economic Co-operation and Development (OECD), are chemicals with at least one saturated  $CF_2$  or  $CF_3$  group, presently comprising over 7 million compounds (Schymanski et al., 2023; OECD, 2021). They have strong carbon-fluorine bonds, resulting in low reactivity and high thermal stability (Buck et al., 2011; ITRC, 2023). Together with water and oil repellency, these properties favored many industrial applications and use in commercial products since the 1940s (Gaines, 2023; Glüge et al., 2020). Their widespread uses and high

environmental stability have led to the omnipresence of PFAS in the environment, potentially presenting a risk to human health and ecosystems (Ahrens & Bundschuh, 2014; ITRC, 2023).

The environmental fate of PFAS is influenced by compound-specific intrinsic properties and external factors. In the aquatic environment, estuaries are subject to high variability of environmental conditions due to tidal cycles, potentially affecting the distribution and bioavailability of PFAS (Anik et al., 2025). Often, industrial and commercial areas are placed near estuaries and threaten these ecosystems with pollution from various sources, including industrial effluents, agriculture, rainwater runoff, and discharges of public and commercial wastewater (Mijangos

<sup>\*</sup> Corresponding author. ECOSPHERE, Department of Biology, University of Antwerp, Groenenborgerlaan 171, 2020, Antwerp, Belgium *E-mail addresses*: musabonso50@gmail.com (M. Bonso), francesca.cappelli@uantwerpen.be (F. Cappelli), fabian.simon@uantwerpen.be (F. Simon), kvo@envs. au.dk (K. Vorkamp), laetitia.six@ovam.be (L. Six), georgios.niarchos@slu.se (G. Niarchos), adrian.covaci@uantwerpen.be (A. Covaci), lieven.bervoets@uantwerpen.be (L. Bervoets), thimo.groffen@uantwerpen.be (T. Groffen).

et al., 2018; Sultan et al., 2024). The tidal flood and ebb currents also result in the distribution and transportation of salts, sediments, nutrients, and (micro)pollutants (Gao et al., 2023; McLusky & Elliott, 2010). Tidal cycles can also resuspend sediments and increase loads of suspended particulate matter (SPM), potentially altering the distribution of PFAS within the estuary (Anik et al., 2025; Liu et al., 2024). Higher salinity near the estuary mouth may reduce the solubility of PFAS in water and increase the adsorption onto sediment and SPM (Liu et al., 2024). As a consequence, bioaccumulation may increase through dietary intake via particle ingestion (i.e., biota-sediment accumulation factor) (Jeon et al., 2010).

Analytical methods for environmental monitoring of PFAS include, among others, target, non-target, and suspect screening techniques (Mu et al., 2024; Rehman et al., 2023; Schlabach et al., 2017). Target methods are optimized for predefined compounds and require a reference standard for identification and quantification. While these methods enable sensitive detection and quantification of a potentially large number of specific PFAS, they will still target only a small subset of known compounds because of the complexity of the PFAS group and the limited availability of analytical reference standards (Rehman et al., 2023; Schlabach et al., 2017; Trier et al., 2025). Non-target analysis (NTA) aims at the identification of unknown compounds without prior assumptions, with the possibility of creating a PFAS fingerprint that extends beyond target analysis (Hollender et al., 2023; Manz et al., 2023). Suspect screening (SS) also operates without analytical standards and identifies compounds by comparing molecular features in a sample to databases of known chemicals to find potential matches. Both SS and NTA are based on high-resolution mass spectrometry, which provides accurate and precise mass spectra as a basis for identifying contaminants of emerging concern in environmental samples (Hollender et al., 2023; Manz et al., 2023).

PFAS pollution has become an issue of concern in media and public discourse worldwide, including in Belgium, following the identification of elevated human serum PFAS levels and environmental concentrations near a hotspot in the vicinity of Antwerp close to the Scheldt Estuary (Groffen et al., 2024). Previous studies also reported high PFAS occurrence in terrestrial environments surrounding the hotspot, including soil and biota (D'Hollander et al., 2014; Groffen et al., 2019a, 2019b; 2023; Lopez-Antia et al., 2019). In aquatic environments, PFAS bioaccumulation has been reported across various species such as Gammarus sp., Asellus sp., and Chironomus sp. (Byns et al., 2024); Chinese mitten crabs (Groffen et al., 2024); European perch (Perca fluviatilis), European eel (Anguilla anguilla), and Dreissena bugensis (Teunen et al., 2021), often exceeding the European Biota Quality Standards (EQS-biota) (Teunen et al., 2021). The Scheldt Basin is known for its high industrial activity, and the estuary serves as a major navigation route for the Port of Antwerp, Europe's second largest seaport. Concerns about estuary pollution have been highlighted previously, for example, related to high concentrations of persistent organic pollutants (POPs) and metals (Van Ael et al., 2012, 2017).

However, studies on the distribution of PFAS in the estuaries remain limited and have generally focused on targeted analysis, which does not reflect the full PFAS complexity and might overlook emerging PFAS, including precursors. Various PFAS precursors and emerging compounds may be present in the estuary, with their distribution and fate potentially influenced by the special environmental conditions of the estuary. Therefore, this study aimed to explore the occurrence of PFAS in the Scheldt Estuary using target analysis, SS, and NTA with the following specific objectives: (1) to investigate the distribution in water, sediments, and bivalves at different locations along the salinity gradient of the estuary; (2) to examine their bioavailability and how it is influenced by sediment and water characteristics; and (3) to assess compliance with the EOS for surface water and biota.

#### 2. Materials and methods

#### 2.1. Study area

The study was conducted along the Scheldt Estuary (51°25′51″N 3°31′44″E; Fig. 1), which extends 160 km inland from its mouth at the North Sea to Ghent, Belgium (Plancke et al., 2023). The estuary has tributaries, including the Rupel and Durme rivers, and is divided into the Western Scheldt and the Sea Scheldt (Zeescheldt). The Western Scheldt stretches 58 km to the Netherlands-Belgium border, while the Sea Scheldt covers 105 km to Ghent (Meire et al., 2005). The sampling sites were both in the Sea Scheldt (i.e., Temse, Schelle, Hemiksem, Steenplein, Zwijndrecht, and Lillo; Fig. 1) and the Western Scheldt (i.e., Hansweert and Hoedekenskerke; Fig. 1). These sites are numbered from upstream to downstream as follows: Temse (S1), Schelle (S2), Hemiksem (S3), Steenplein (S4), Zwijndrecht (S5), Lillo (S6), Hansweert (S7), and Hoedekenskerke (S8). Adjacent to the estuary at Zwijndrecht (S5), there is a fluorochemical plant in Antwerp (3M) that has been producing PFAS since 1976 (3M Company, 2022).

The estuary has a mean depth ranging from approximately 10 m at S1 to 25 m at the estuary mouth. The average tidal range is approximately 3.8 m at the estuary mouth and increases to approximately 5.8 m at S1 (Meire et al., 2005). The geomorphology of the estuary is characterized by a network of flood and ebb channels covering large intertidal sand and mud flats in the Western Scheldt, followed by a narrower and single tidal channel in the Sea Scheldt. Due to tidal asymmetry, sediment is transported more upstream during high tide, leading to sediment accumulation in the upper part of the estuary (Plancke et al., 2023). The turbidity maximum zone varies seasonally, extending up to approximately 50 and 110 km from the estuary mouth during the winter season and dry summer, respectively (Meire et al., 2005). The estuary has great ecological importance, serving as a habitat for water birds and migrating fish species, and provides other ecosystem services. In addition, the estuary has significant economic importance and has a densely populated catchment area, with approximately 500,000 and 250,000 inhabitants in the cities of Antwerp and Ghent, respectively, and a long industrial tradition (Plancke et al., 2023).

# 2.2. Sample collection and field exposure

## 2.2.1. Test organisms

The study utilized bivalve mollusks, Asian clams (*Corbicula fluminea*) and blue mussels (*Mytilus edulis*), as test organisms. The Asian clam is an invasive species known for its ability to easily colonize new environments due to its rapid growth, short lifespan, early sexual maturity, and high reproductive capacity (McMahon, 2002). It can be used as an indicator species for micropollutants in aquatic environments, given its wide distribution, broad salinity tolerance (from fresh to brackish water), adaptability to translocation and laboratory conditions, resilience in both pristine and contaminated habitats, and significant filtration capacity (McMahon, 2002). Several studies have demonstrated the reliability of Asian clams in monitoring PFAS pollution (Guo et al., 2019, 2023; Koban et al., 2024; Teunen et al., 2021).

Similarly, resident blue mussels (*Mytilus edulis*) are efficient filter feeders and are widely used in environmental pollution monitoring programs, such as the Mussel Watch program, which operates in over 50 countries worldwide (Beyer et al., 2017). Blue mussels have been used for monitoring trace metals and organic micropollutants, including PFAS (Beyer et al., 2017; Bråte et al., 2018). Their suitability arises from their widespread presence in temperate coastal areas and sessile nature, providing location-specific information. In addition, they are easy to collect and simple to maintain in culture, making them ideal for translocation and caging exposure experiments (Bråte et al., 2018). In this study, Asian clams were used at the brackish stations (S1-S6; Fig. 1), whereas blue mussels were used at the stations with higher salinity (S7-S8; Fig. 1).

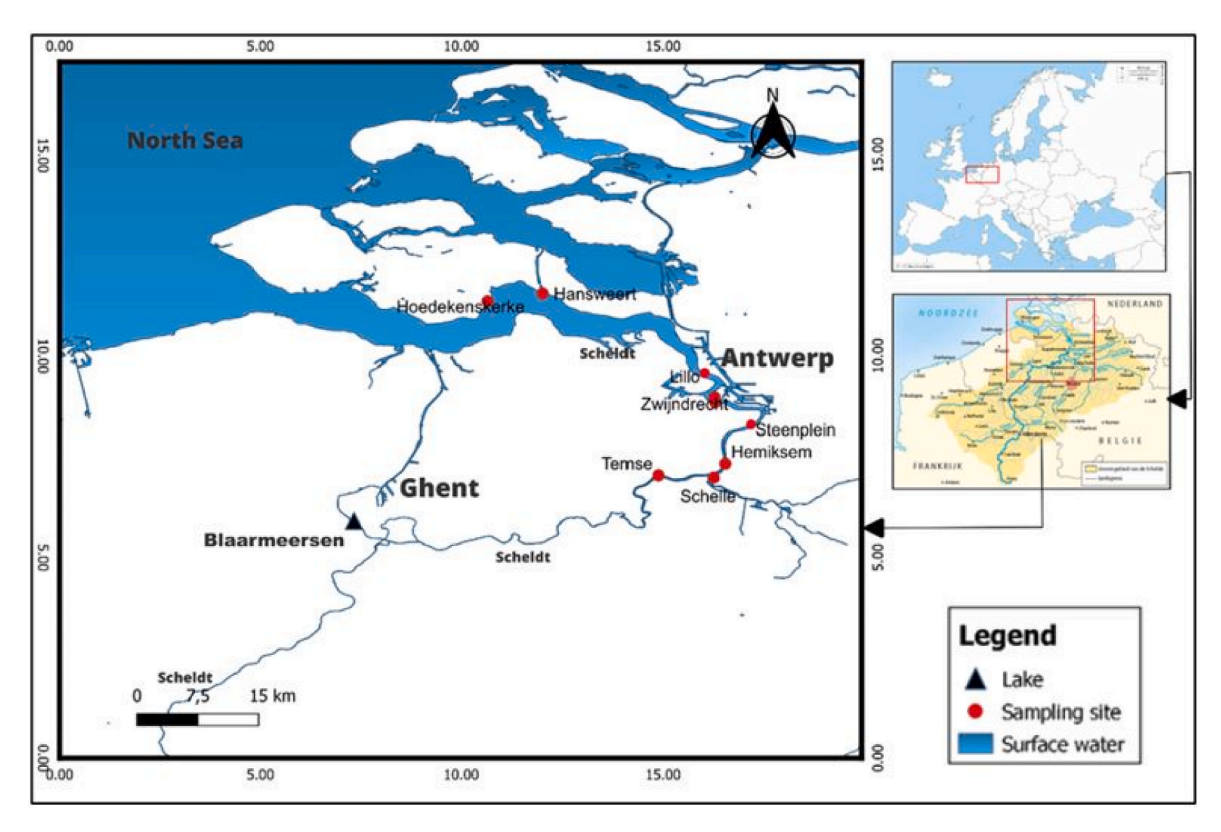


Fig. 1. Map of study area and sampling sites along the Scheldt Estuary (made by Alain Mugisho and used with permission). The sites are shown from upstream to downstream as follows: Temse (S1), Schelle (S2), Hemiksem (S3), Steenplein (S4), Zwijndrecht (S5), Lillo (S6), Hansweert (S7), and Hoedekenskerke (S8).

## 2.2.2. Field exposure

Asian clams were sampled from Blaarmeersen Lake in Ghent in September 2023, chosen for its absence of known pollution sources (Bervoets et al., 2005; Byns et al., 2024; Teunen et al., 2021), and acclimated for 3 weeks at the University of Antwerp mesocosm facility. After the acclimation period, the clams were translocated to six locations along the salinity gradient of the Sea Scheldt part of the estuary (S1-S6; Fig. 1). The detailed protocol for Asian clam translocation was described by Bonso et al. (2025) and is detailed in supplementary information (Text S1). A total of 30 clams were taken from the mesodrome and distributed across the locations (five per location, n = 6 locations), where they were exposed for six weeks and subsequently recollected for PFAS analysis, including target analysis and SS/NTA. Additionally, pre-exposure PFAS concentrations were analysed in five clams taken directly from the mesodrome. To assess concentrations downstream in the Western Scheldt, resident blue mussels (five per location) were analysed for PFAS from S7 and S8 locations, since Asian clams cannot survive in saline water. Although comparing the concentrations in resident and transplanted organisms may not be ideal, previous studies have shown that concentrations of metals and organohalogenated compounds in translocated zebra mussels were comparable with those in resident organisms within a six-week exposure period (Bervoets et al., 2004; Teunen et al., 2021). In addition, no substantial differences in PFAS profiles were observed between translocated and resident mussels (Teunen et al., 2021).

Three abiotic sampling campaigns were conducted at three different time points throughout the 6-week exposure period: on September 25, 2023 (the first day of exposure of Asian clams), October 25, 2023, and November 6, 2023 (during the collection of the exposed clams). Water samples were collected from approximately <15 cm below the water surface using a plastic bucket at the waterbus docking pontoons and transferred to 50 mL polypropylene (PP) tubes by submerging the tubes into the bucket. A total of 24 water samples were collected and analysed with target analysis, with three samples (1 per time point) taken from

each of the eight locations investigated. Sediment samples were obtained with a Petit Ponar grab sampler (Wildco cat. no. 1782; 235 cm²) from the sediment surface at a depth of approximately <10 cm and transferred to 50 mL PP tubes. Similarly, three sediment samples per location were collected and analysed (1 per time point), resulting in a total of 24 sediment samples. Average PFAS concentrations of the three water or sediment samples over time thus represent averages across the exposure period of the bivalves. For the SS and NTA, only one sample was analysed for water and sediment per location, while five replicates were analysed for bivalves per location. Detailed information on the sampling and sampling sites is summarized in Table S1 of the supplementary information. All samples were transported to the laboratory immediately after sampling, stored at -20 °C, and extracted within three weeks after collection.

## 2.3. Water and sediment physicochemical characteristics

Water samples were analysed on-site using a multimeter (HQ30d, Hach, Loveland, Colorado, United States) to measure dissolved oxygen (DO; mg/L), pH, conductivity ( $\mu$ S/cm), and temperature (°C). Each variable was measured twice during each of the three sampling times, and the averages for all three sampling times were calculated (Table S2). Sediment total organic carbon (TOC) was determined by combustion in a muffle furnace, following the protocols by Heiri et al. (2001) (Text S2). In addition, the sediment clay content (particles with a size <2  $\mu$ m) was measured using a Malvern Mastersizer 2000 equipped with a Hydro 2000G unit (Text S2).

## 2.4. PFAS analysis

### 2.4.1. Chemical extractions

The extraction of water and sediment was performed following the protocol by Groffen et al. (2019c). Water samples were analysed without filtration, thus representing bulk concentrations that include both

dissolved PFAS and those adsorbed to SPM. For the extraction of water samples, solid-phase extraction (SPE) cartridges were used. Suspended matter was trapped on top of the sorbent material and did not compromise cartridge performance. The extraction of mussel and clam samples followed the protocol by Powley et al. (2005). Bivalves were not depurated prior to extraction, as the main interest was on body burdens under these exposure conditions. Details on the sample chemical extraction procedures are provided as supplementary information (Text S3).

## 2.4.2. Instrumental analysis, compound identification and semiquantification

Target analysis of PFAS was conducted using ultra-performance liquid chromatography-tandem mass spectrometry (UPLC-MS/MS; ACQUITY TQD, Waters, Milford, MA, USA) operated in electrospray negative ionization mode (ESI-). A total of 29 PFAS were included in the target analysis. A list of compounds and analytical details used for quantification is given in Table S3 and Text S4 of the supplementary information. SS and NTA were performed using a 1290 ultra-high-performance liquid chromatography (UHPLC; Agilent Technologies, Santa Clara, CA, USA) coupled with a 6530 Q-TOF mass spectrometer with an Agilent Jet Stream electrospray ionization source (AJS ESI; Agilent, Santa Clara, CA, USA). Details on the instrumental settings are provided in the supplementary information (Text S4).

Data analysis of the input raw data from SS and NTA (.d files) began with conversion to.mzML format using MSConvert from ProteoWizard, followed by MZmine 4.3 for feature extraction. In addition, mass defect filtering (-0.25-0.1) was used, and blank subtraction was based on selecting peaks whose areas exceeded those of the blanks by a 3-fold change. Filtered results were matched against two libraries, namely the PFAS Master List of the United States Environmental Protection Agency (USEPA) CompTox and PFASNTREV19 (Liu et al., 2019), covering more than 10,000 PFAS and including several homologue series. For compound annotation, the [M-H] adduct was used and only features with a mass tolerance of  $\pm 5$  ppm between the suspect compound detected in the sample and the corresponding library entry were retained for further confirmation. These suspect compounds were subsequently injected in target-MS/MS mode to acquire the MS/MS spectra and confirm the fragmentation pattern, using in-silico tools (e.g., Met-Frag, ACD/MS Fragmenter) and by identifying diagnostic fragments (Text S4). A schematic flowchart has been added to the supplementary material (Fig. S1). In addition to the MZmine workflow, an in-house Python code was used to search for PFAS-specific diagnostic fragments in auto MS/MS.mzML files with a mass tolerance of 5 mDa. The same diagnostic fragment list as described for the PFAScreen software was used (Zweigle et al., 2024). Therefore, peak shapes, retention times, and MS/MS plausibility were checked manually while blank correction (3-fold change) and mass defect filtering (MD range: 0.25-0.1) were automatically processed. Identified MS1 peaks were compared with the suspect list within a mass tolerance of 5 mDa and subsequently checked for in-silico fragmentation via MetFrag. The confidence level (CL) of a compound was determined based on Charbonnet et al. (2022).

Semi-quantification of the identified compounds (at CL1 to CL3) was performed using a commercial software (https://quantem.co/), which predicts the ionization efficiency (IE) of suspect and non-target PFAS to estimate their concentrations. The model, based on Mordred 2D molecular descriptors (Moriwaki et al., 2018), was trained on IE values from 80 PFAS compounds analysed across different instruments and conditions, following the approach of Lauria et al. (2024). Model performance showed an average estimation error of approximately two-fold, with the 95th percentile error reaching up to four-fold between predicted and measured PFAS concentrations. The Quantem analytics software uses so-called "tailoring compounds," which are compounds that were measured under the same conditions as analytes with known concentrations. Quantem needs tailoring compounds to make concentration predictions specific to the applied analysis conditions. Therefore,

for semi-quantification of bivalves, water, and sediment non-target compounds, 58 tailoring compounds were added into the analysis scheme, consisting of PFAS standard substances taken from the target list.

### 2.4.3. Quality assurance and control

Procedural blanks involved 10 mL of acetonitrile (ACN) for bivalves and sediment and 10 mL of Milli-Q water (MQ) for water samples treated in the same way as the samples. For every 10 samples, one procedural blank was used. Instrumental blanks involved injecting 100 % ACN regularly to prevent crossover contamination. Limit of quantifications (LOQs) were established in the matrix as concentrations corresponding to a signal-to-noise ratio (S/N) of 10 (Table S4). The recoveries of the internal standards for target analysis were 81-96 %.

To test the applicability of the model used for semi-quantification, we used our own analytical standards that were available for perfluorohexane sulfonamide (PFHxSA), perfluorooctanesulfonamide (PFOSA), and N-methylperfluorooctanesulfonamidoacetic acid (N-MeFOSAA) based on the calibration standards that were injected within the same sequence as the samples. The results for bivalve samples (Fig. S2) showed a similar trend of concentration levels between the two semi-quantification approaches. However, the Quantem analytics software approach determined systematically higher concentrations (about 10-20 %) compared to our in-house method. Therefore, in the scope of the analysed compounds, a minor overestimation of the semi-quantified values can be expected, while the comparison of the Quantem analytics and in-house semi-quantification approaches showed compatibility.

#### 2.5. Bioaccumulation factor and biota-sediment accumulation factors

The Bioaccumulation Factor (BAF) assesses the combined uptake of PFAS via several pathways, including water and dietary sources, describing the net result of absorption, distribution, metabolism, and excretion (Arnot & Gobas, 2006). In this study, BAFs were calculated as the ratio of PFAS concentration in the organism to the concentration in the water (Formula 1), since no dietary information was available. The Biota-Sediment Accumulation Factor (BSAF, Formula 2) estimates the accumulation of PFAS in organisms from sediment, defined as the ratio of concentration in biota to a concentration in sediment (Arnot & Gobas, 2006).

$$BAF_{Bivalves; Scheldt Estuary} = C_b/C_w$$
 (1)

$$BSAF_{Bivalves; Scheldt Estuary} = C_b/C_s$$
 (2)

Where BAF represent the Bioaccumulation Factor (L/kg) of this study, BSAF the Biota-Sediment Accumulation Factor (kg/kg),  $C_b$  the concentration of PFAS in bivalves (ng/g wet weight (ww)),  $C_s$  the concentration of PFAS in sediment (ng/g dry weight (dw)), and  $C_w$  the concentration of PFAS in water (ng/L).

A BAF and BSAF >1 means that the PFAS concentration in bivalves is higher than the concentrations in water and sediment, respectively, showing that at the time of sampling, the uptake and absorption of a given PFAS exceed the excretion of this substance, potentially indicating bioaccumulation. While the clams were not directly in contact with the sediment, they might still be exposed to sediment-associated PFAS in the dynamic tidal environment where sediment particles are suspended in the water column and redistributions between particles and water might occur.

## 2.6. Statistical analysis

Out of the 29 target analytes, 13 PFAS were detected in at least one of the water, sediment, and bivalve samples. These included perfluorobutanoic acid (PFBA), perfluorobutane sulfonate (PFBS), perfluorohexanoic acid (PFHxA), perfluorooctanoic acid (PFOA), perfluorooctane sulfonate (PFOS), perfluorononanoic acid (PFNA), perfluorodecanoic acid (PFDA), perfluorodecanoic acid (PFDDA), perfluorotridecanoic acid (PFTrDA), perfluorotetradecanoic acid (PFTeDA), perfluoro-4-oxapentanoic acid (PF4OPeA), perfluorobutane sulfonamide (FBSA), and 6:2 fluorotelomer sulfonate (FTS) (Fig. S3, Table S5).

Furthermore, only compounds having at least a 30 % detection frequency were included in the statistical analysis to ensure the validity assumption of a normal distribution (Groffen et al., 2024) and to balance inclusion of less frequently detected PFAS with statistical power. This excluded some of the detected compounds from the statistical analysis of the matrix-specific results, as specified in section 3. Prior to statistical analysis, PFAS concentrations that were < LOQ were substituted with numerical values through Maximum Likelihood Estimation (MLE) (Villanueva, 2005). The significance level for the statistical analysis was established at p  $\leq$  0.05.

In computing the sum  $(\sum)$  of PFAS concentrations, values < LOQ were substituted with zero. The relative contribution of each individual PFAS to  $\sum$ PFAS was calculated by accounting for their molecular weight. Shapiro-Wilk tests were used to examine the assumptions of normality of the dataset. Outliers were determined using the Grubbs test and, upon detection, excluded before conducting the analyses. One-way ANOVA and Kruskal-Wallis tests were performed to identify variations in the concentrations detected in water, sediment, and bivalves at different locations. Additionally, correlation and multiple regression analysis were conducted to examine the relationship between environmental concentrations and their accumulation in bivalves, considering sediment and water characteristics. Moreover, Principal Component Analysis (PCA) was performed to identify correlations among  $\sum$ PFAS and abiotic characteristics such as TOC, clay content, and conductivity, as well as among their concentrations in the abiotic environment.

### 3. Results and discussion

#### 3.1. PFAS concentrations in water and spatial distribution

Target analysis detected a total of 8 PFAS above the LOQ in at least one water sample. These included the short-chain PFAS (PFBA and PFBS), long-chain PFAS (PFOA, PFOS, PFNA, and PFTrDA), and the potential precursors PF4OPeA and 6:2 FTS (Figs. S3–S4; Table S5). For the statistical analysis, only PFBA, PFOA, and PFOS were considered, given their detection in  $\geq$ 30 % of the samples.

Comparing among locations, only PFOA showed significant differences (p < 0.05). Its highest mean concentrations were detected at S4 (22.3  $\pm$  5.9 ng/L) and S7 (21  $\pm$  3.6 ng/L). The lowest concentration was detected at S8 (3.6  $\pm$  4.4 ng/L), which was significantly lower than the concentrations at sites S1-S7 (Fig. S4; Table S5). The concentration of PFOS was highest at S2 (17.4  $\pm$  23 ng/L), while it was < LOQ at S4 and S8. The short-chain PFAS PFBA had its highest mean concentration of 93.5  $\pm$  60 ng/L at S4, whereas it was < LOQ at S8. At the locations detected above the LOQ, PFBA concentration was higher than the long-chain PFAS, such as PFOS, PFOA, and PFNA. However, its concentration was exceeded by the long-chain compound PFTrDA (183  $\pm$  175 ng/L) at S3 and 6:2 FTS (58  $\pm$  98 ng/L) at S5 (Fig. S4; Table S5).

There has been an increase in both the detection frequency and concentrations of short-chain PFAS, such as PFBS and PFBA, in approximately the last 15 years, likely due to the replacement of long-chain PFAS with short-chain hydrophilic and presumably less bio-accumulative alternatives (Kurwadkar et al., 2022; Podder et al., 2021). In the present study, the concentration of PFBA was the highest in water at most locations. Likewise, other studies have reported the dominance of short-chain PFAS concentrations in water (Koban et al., 2024; Lenka et al., 2022). Over the past two decades, concentrations of PFOA and PFOS in European surface waters have been within the range of 10–100 ng/L (Podder et al., 2021). In our study, mean PFOS concentrations were

at the lower end of this range (<LOQ-17.4 ng/L), but they still exceeded the inland surface water EQS of 0.65 ng/L (EU, 2013; Flemish environmental agency, 2018) at all sites, except at S4 and S8.

The highest mean ∑PFAS concentration in the target analysis was detected at S7 (585 ng/L), with 97.5 % attributed to PFBS (Fig. 2a and b). This short-chain compound was only detected at the Western Scheldt (i.e., S7 and S8), with the highest mean concentration of 538.3 ng/L at S8. These sites may be influenced by wastewater discharges from nearby treatment plants, such as Willem-Annapolder and Waarde in the Netherlands. Inefficient removal and biodegradation of precursor compounds during wastewater treatment processes likely result in PFAS released into the Western Scheldt (Waterschap Scheldestromen, 2024). In the Sea Scheldt region, the highest mean  $\sum$  PFAS concentration was at S3 (294 ng/L; Fig. 2a), with PFTrDA accounting for the highest relative contribution of 44 % (Fig. 2b). This may be attributed to the resuspension of PFAS from sediment, which may be strongest around this location as a consequence of tidal dynamics. The site is situated near the turbidity maximum zone, which extends 110 km from the mouth during dry periods (Meire et al., 2005). As the water samples were not filtered prior to analysis, PFAS adsorbed on SPM are included in the total water concentrations results. Long-chain PFAS such as PFTrDA are more likely to adsorb to SPM than the short-chain PFAS.

SS and NTA of water samples annotated 7 PFAS as CL1-CL4, based on exact mass matching, isotopic patterns, and available MS/MS fragmentation (Fig. S3; Table S6). Three compounds were detected at CL1a, i.e., confirmed with an analytical standard: trifluoromethanesulfonic acid (TFMS), N-methylperfluorohexane sulfonamido acetic acid (N-Me-PFHxSAA), and PFOSA. In addition, three compounds, including 2,2,3,3-tetrafluorocyclopropane-1-carboxylic acid (TFCPrA), N-(4-(2-(2-aminopyridin-4-yl)thiazol-5-yl)-3-chlorophenyl)-1,1,1-trifluoromethanesulfonamide (APTTFMS), and 2-(N-methylperfluorooctanesulfonamido)-acetic acid (N-Me-PFOSAA), were detected at CL3b, CL3c, and CL3d, respectively (Table S6). The compound 1-propa-3-((3,3,4,4,5,5,6,6,7,7,8,8,9,9,10,10,10-heptadecafluorodecyl) thio)- (C<sub>13</sub>H<sub>11</sub>F<sub>17</sub>OS) was detected at CL4. Interestingly, while the precursor N-Me-PFHxSAA was detected, we did not detect perfluorohexane sulfonic acid (PFHxS) or PFHxA, which would be transformation products of N-Me-PFHxSAA, in the water samples of this study. This might indicate recent emissions of N-MePFHxSAA, but it can also be influenced by the analytical method, which had slightly higher LOQs for PFHxS and PFHxA than for example PFOA (Table S4).

The semi-quantitative concentrations of PFAS detected through SS and NTA were determined for all except  $C_{13}H_{11}F_{17}OS$  (Table S7). Among these, the estimated concentration of TFMS was highest at S5 (4520 ng/L; Table S7). Additionally, TFMS was the dominant PFAS in terms of its contribution to the estimated  $\sum$ PFAS at most locations (Fig. 2d). On the other hand, APTTFMS was estimated to be highest at S7 (1685 ng/L) and S5 (1385 ng/L), and it was the dominant contributor to the estimated  $\sum$ PFAS concentrations at S1 and S7 (Table S7; Fig. 2d). The estimated  $\sum$ PFAS concentration at S5 (6421 ng/L), mainly dominated by TFMS, was found to be approximately 3-fold higher than the estimated  $\sum$ PFAS concentrations at the other locations (Fig. 2c).

TFMS has been reported in surface water and groundwater in Europe, with concentrations reaching up to 1000 ng/L (Björnsdotter et al., 2019; Schulze et al., 2019). In the present study, the estimated concentration of TFMS at S5 (where the 3M company is located) was found four times higher than the levels found in other European countries (Björnsdotter et al., 2019; Schulze et al., 2019). This concentration was also 4 to 40 times higher than the estimated concentration at other sites of this study, indicating the presence of sources of TFMS at this location. Furthermore, TFMS was detected in drinking water collected from Antwerp City and its surrounding areas in Belgium, with concentrations reaching up to 15 ng/L (Cappelli et al., 2024). The potential sources of TFMS remain unclear but might be related to its use in polymerization processes in industries (Björnsdotter et al., 2019; Schulze et al., 2019). In the present study, only TFMS was detected

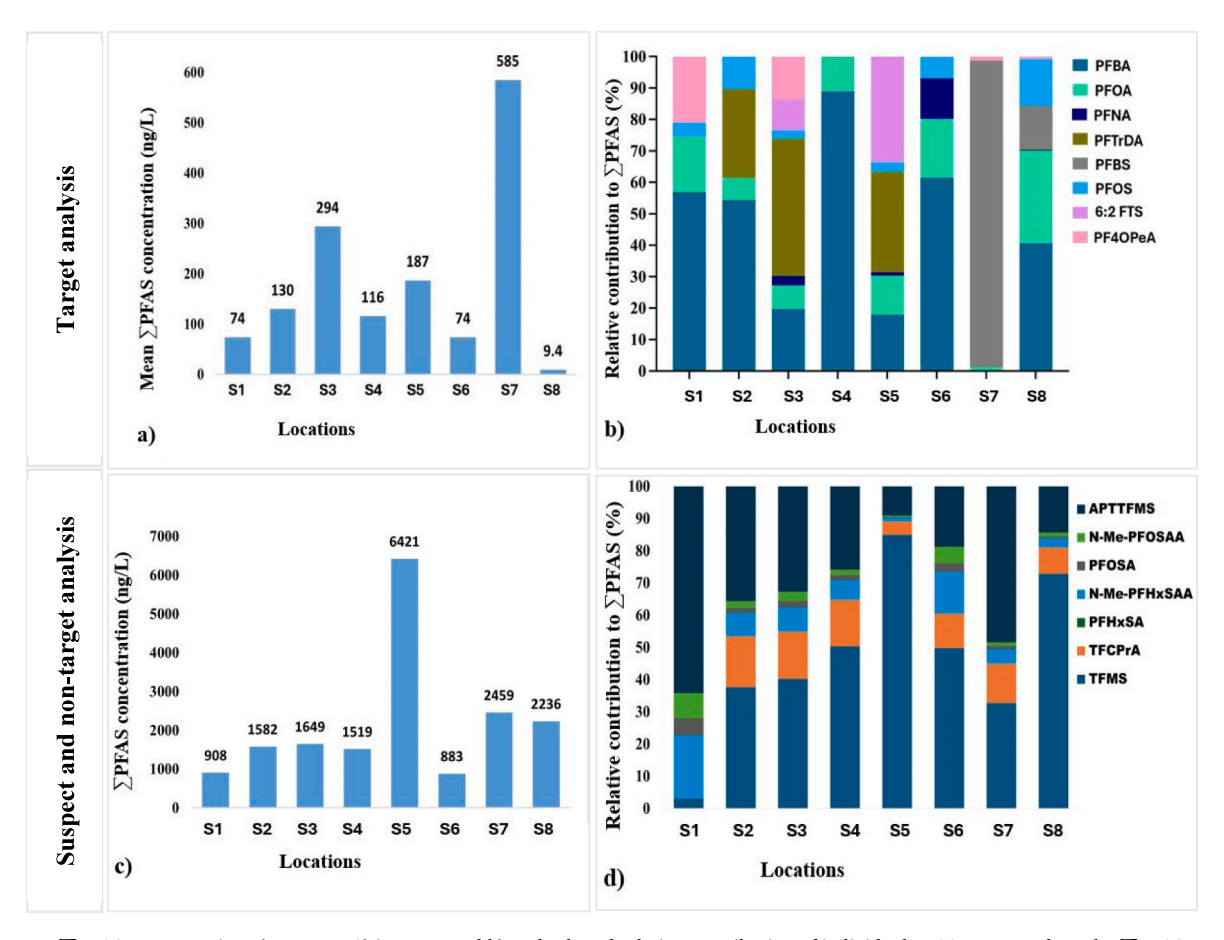


Fig. 2. a) Mean  $\sum$ PFAS concentrations (ng/L; n=3) in water and b) molar-based relative contribution of individual PFAS compounds to the  $\sum$ PFAS concentration investigated by target analysis; c) estimated  $\sum$ PFAS concentrations through semi-quantification (ng/L; n=1) and d) molar-based relative contribution of individual PFAS to the estimated  $\sum$ PFAS concentration profile at each location investigated by suspect and non-target analysis.

among the ultra-short-chain PFAS; however, this might be influenced by the analytical method. The high polarity of ultra-short-chain PFAS may result in poor retention on C18 reversed-phase columns, likely limiting their detection. The pattern of ultrashort- and short-chain PFAS predominating water samples may be caused by their high solubility and mobility in water. Other detected compounds include PFOSA, which is a precursor to PFOS (Zhang et al., 2025). Compounds, such as N-Me-PFHxSAA and N-Me-PFOSAA, are intermediate degradation products of electrochemical fluorination-based surfactants and polymers, which can eventually be transformed to perfluoroalkyl sulfonic acids (PFSAs) and perfluorocarboxylic acids (PFCAs) (ITRC, 2023).

#### 3.2. PFAS concentration in sediment and spatial distribution

In the sediment samples, 11 PFAS compounds were detected above the LOQ in at least one sample through target analysis. These detections included short-chain PFAS (PFBA and PFHxA), long-chain PFAS (PFOA, PFOS, PFNA, PFDA, PFDODA, and PFTrDA), and the potential precursors FBSA, PF4OPeA, and 6:2 FTS (Figs. S3 and S5; Table S5). Among these, PFHxA, FBSA, PFDA, and PFDoDA, although present in sediment, were not detected above the LOQ in any water sample. Conversely, PFBS, which was found at elevated concentrations in water from the Western Scheldt, was not detected above the LOQ in sediment at any location. For the statistical analysis, PFNA, PFDA, and PFTrDA were omitted due to detection frequency <30 %. No significant differences were observed between locations in the mean concentrations of the remaining PFAS (p > 0.05).

The distribution of the short-chain PFAS, PFBA and PFHxA, was similar across sites (Fig. S5), with the highest mean concentrations at S6

(4.6  $\pm$  3.9 and 4.7  $\pm$  4.3 ng/g dw, respectively), followed by S1 (3.3  $\pm$ 1.6 and 3.7  $\pm$  1.7 ng/g dw, respectively), and the lowest at S7 (2.05  $\pm$ 1.4 and 0.63  $\pm$  0.8 ng/g dw, respectively). Similarly, FBSA, a potential precursor of PFBS, showed its highest concentration at S6 (8.3  $\pm$  5.4 ng/ g dw), followed by S1 (7.9  $\pm$  1.8 ng/g dw), while the lowest concentration was found at S7 (0.9  $\pm$  1.2 ng/g dw). Previous studies had also detected PFBA and PFHxA in sediments (e.g., Groffen et al., 2024; Koban et al., 2024), which may be related to the release of short-chain PFAS due to the industrial shift towards these alternatives, as also discussed for the water samples. Given the hydrophilicity of the short-chain PFAS, they might be present in pore water rather than being attached to particles, but this was not distinguished in our analyses. The transformation of precursors, such as 6:2 FTS, in sediment could also contribute to these detected short-chain PFAS (Yan et al., 2024). The compound FBSA has only recently been reported in sediment, and it is both a degradation product and a major metabolite of several precursor compounds (Zhong et al., 2021). This compound was reported to have been produced by 3M and detected in the Scheldt, according to media reports (VRT.be, 2021).

Long-chain PFAS had higher percentages in the composition profiles of sediment than in the corresponding water profiles. This was expected due to their higher hydrophobicity and stronger sorption to sediment. As PFAS chain length increases, the partition coefficient between the solid phase and water ( $K_d$ ) increases, indicating a higher tendency of partitioning to sediment (Buck et al., 2011; ITRC, 2023). Despite the phase-out of PFOS and PFOA, relatively high concentrations of these compounds were detected at site S5, where the 3M company is located. The highest average PFOA concentration was detected at S5 and S7, with a mean concentration of  $1.04 \pm 0.4$  and  $1.1 \pm 1.05$  ng/g dw, respectively. The highest mean PFOS concentration was at S2 ( $2.1 \pm 3.2$ 

ng/g dw), followed by S5 (1.6  $\pm$  0.6 ng/g dw). In addition, a relatively high concentration of PFTrDA was observed at S5, probably due to the proximity of the 3M site.

The highest mean  $\sum$ PFAS concentration from target analysis was detected at S3 (47.8 ng/g dw), with the highest contribution of the precursor 6:2 FTS (Fig. 3a and b). This location also had the highest mean  $\sum$ PFAS concentration in water among the Sea Scheldt locations. As discussed before, this may be attributed to tidal dynamics, where PFAS can be transported upstream with the tides from hotspot areas. During this transport along the estuary, PFAS may become adsorbed onto sediment and particulate matter within turbidity maximum zones, where freshwater meets saline water, leading to increased sediment deposition and higher accumulation of PFAS. In contrast to the  $\sum$ PFAS concentration in water, the lowest mean  $\sum$ PFAS concentration in sediment was detected at S7 (7.5 ng/g dw) (Fig. 3a).

PFBA and FBSA had the highest contributions to the  $\sum$ PFAS concentrations at most sediment locations, potentially related to their occurrence in porewater rather than adsorption to particles (Fig. 3b). Specifically, FBSA accounted for 40 %, 36 %, and 35 % of the total PFAS at S2, S6, and S1, respectively. Additionally, the contribution of PFBA was observed to increase downstream with 22 %, 28 %, 35 %, and 39 % of the total PFAS profile at S5, S6, S8, and S7, respectively (Fig. 3b). Moreover, these short-chain PFAS (i.e., PFBA, PFHxA, and FBSA) accounted for 66 % of the total  $\sum$ PFAS concentrations detected through target analysis at most locations.

SS and NTA screening of sediment samples identified 8 compounds not included in the target analysis at CL1-CL4 (Fig. S3; Table S6). Among these, 3,3,4,4,5,5,6,6,6-nonafluorohexyl thiocyanate ( $C_7H_4F_9NS$ ) and PFHxSA were not detected in the water samples. Semi-quantification was conducted for all compounds except for  $C_7H_4F_9NS$  and

 $C_{13}H_{11}F_{17}OS$ . The estimated  $\sum$ PFAS concentrations were highest at S8 (110 ng/g dw) and S3 (97 ng/g dw) (Fig. 3c). At all locations, PFOSA was the dominant contributor to the estimated  $\sum$ PFAS concentration in sediment, with the highest estimated PFOSA concentration of 100 ng/g dw at S8 (Fig. 3d; Table S7). PFOSA, a known PFOS precursor, was widely used in industrial processes, including the production of surfactants and surface treatment agents (Zhang et al., 2025).

### 3.3. PFAS concentration in bivalves and spatial distribution

The highest mean PFBS concentration was observed at S4 (15.6  $\pm$  7.8 ng/g ww), significantly exceeding concentrations detected at S1 (0.8  $\pm$  1.7 ng/g ww), S6 (2.3  $\pm$  4.9 ng/g ww), S7 (8.8  $\pm$  2.4 ng/g ww), and S8 (9.7  $\pm$  7.3 ng/g ww) (Fig. S6; Table S5). However, at S4, PFBS was < LOQ in both water and sediment, while at S7 and S8, it aligned with the concentrations found in water. Furthermore, sites S5 and S7 had the highest mean concentrations of long-chain PFAS in bivalves, including PFOS, PFOA, and PFTrDA. The mean concentration of PFOS was 1.17  $\pm$  1.25 ng/g ww at S5 and 0.8  $\pm$  0.3 ng/g ww at S7, both significantly higher than concentrations at S2 (0.34  $\pm$  0.7 ng/g ww) and S6 (0.24  $\pm$ 

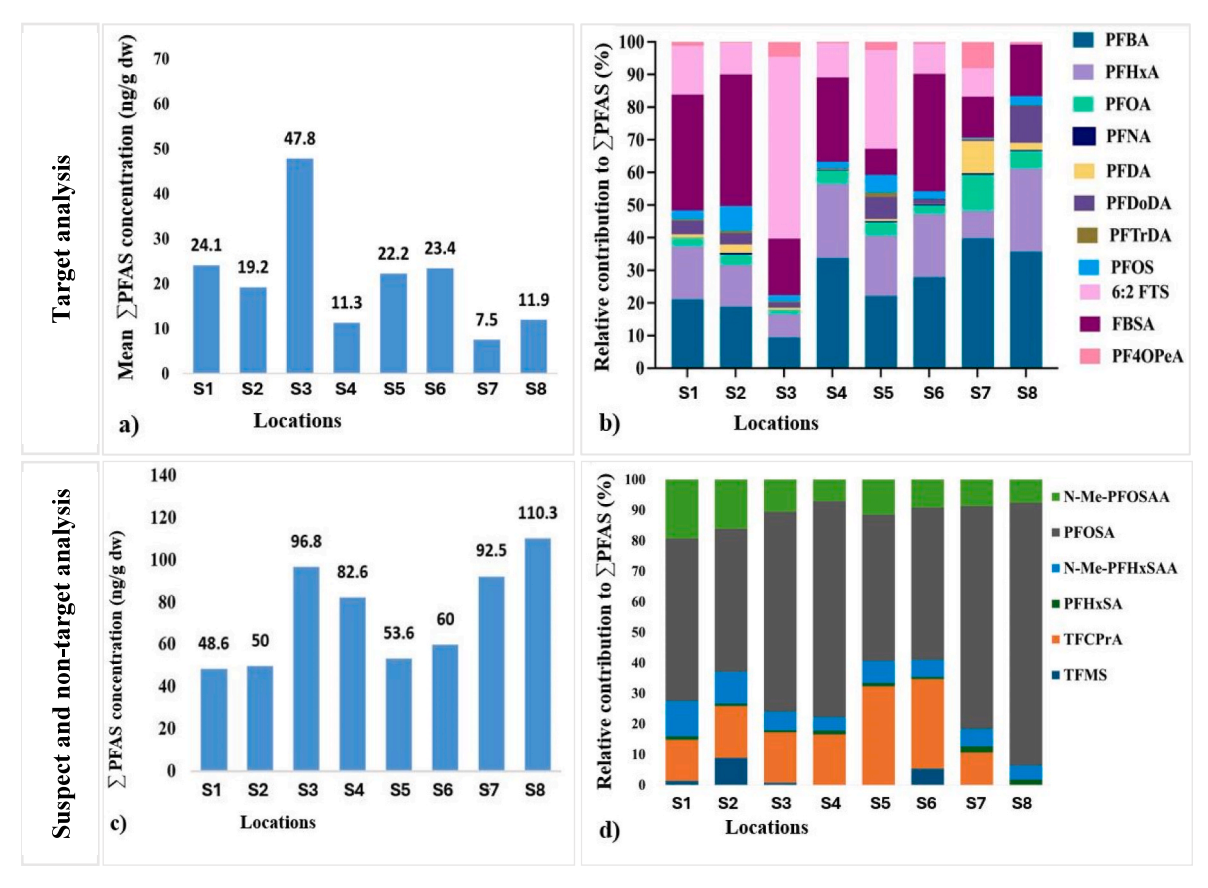


Fig. 3. a) Mean  $\sum$ PFAS concentrations (ng/g dw; n = 3) in sediment and b) molar-based relative contribution of individual PFAS to the  $\sum$ PFAS concentration by target analysis; c) estimated  $\sum$ PFAS concentrations through semi-quantification (ng/g dw; n = 1) and d) molar-based relative contribution of individual PFAS to the estimated  $\sum$ PFAS concentration profile (100 %) at each location investigated by suspect and non-target analysis.

0.3 ng/g ww) (p < 0.05). The mean concentrations of PFTrDA at S5 (1.4  $\pm$  1.3 ng/g ww) and S7 (1.2  $\pm$  0.72 ng/g ww) were significantly higher than concentrations at S8 (0.45  $\pm$  0.47 ng/g ww) and S1 (0.57  $\pm$  1.2 ng/g ww) (p < 0.05). The mean concentration of PFOA was 0.8  $\pm$  0.7 ng/g ww at S5 and 0.77  $\pm$  0.36 ng/g ww at S7 (Fig. S6; Table S5).

Bioaccumulation of PFAS is influenced by both the carbon chain length and the type of anionic functional group. Regarding functional groups, PFSAs are typically more bioaccumulative than PFCAs of the same chain length, yet both types with eight or more fluorinated carbons have high bioaccumulation potential (ITRC, 2023). In contrast, the potential for accumulation is comparatively lower for shorter-chain PFAS (Brendel et al., 2018). The presence of short-chain PFAS in bivalves of this study may be reflective of the continuous exposure and resulting uptake at the study sites. A previous study had also detected short-chain PFAS (e.g., PFHxA), PFPeA, and long-chain PFAS (e.g., PFOA, PFDA, PFDODA, and PFTeDA) in bivalves along the Scheldt estuary (Teunen et al., 2021).

In particular, high accumulation of PFOS and PFOA had been reported at S5 (Teunen et al., 2021). Additionally, PFTrDA was also the highest at S5, both in bivalves and sediments, suggesting historical use, though the direct source was unknown. However, the concentrations of PFTrDA detected in this study were much lower than the concentrations reported along the Belgian coast of the North Sea, where concentrations ranged from <LOQ to 116 ng/g ww (Byns et al., 2022). This difference may be attributed to variations in species used for monitoring and pollution sources. The mean PFOS concentrations in bivalves of this study (<LOQ-1.17 ng/g ww) were also below the EQS-biota of 9.1 ng/g ww (EU, 2013; Flemish environmental agency, 2018).

PFBS concentrations in bivalves were observed to increase

downstream, which is in line with PFBS concentrations in water. The PFBS occurrence in bivalves was likely related to the exposure to wastewater discharged from industrial activities, as described in the water section. Additionally, the occurrence of potential precursors, such as FBSA, may explain the concentration of PFBS in bivalves. FBSA had also been detected in muscle samples of flounder (*Platichthys flesus*) from the Western Scheldt, with a concentration of 80.1 ng/g ww (Chu et al., 2016). Another short-chain compound, PFBA, was also detected at all examined locations in the current study, in both water and bivalves.

In terms of mean ∑PFAS concentrations measured by target analysis, clams at S4 had the highest concentrations (17.5 ng/g ww), followed by S8 (16 ng/g ww) and S7 (12 ng/g ww), where resident blue mussels were analysed (Fig. 4a). This was mainly attributed to the significant contribution of short-chain PFBS, accounting for 91 %, 76 %, and 70 % of  $\Sigma$ PFAS at S4, S7, and S8, respectively (Fig. 4b). The high concentration at S4 could be attributed to industrial activity, including that at the Port of Antwerp. Although the concentrations of  $\Sigma$ PFAS in the abiotic environment were highest at S3, the accumulated concentration in bivalves was found to be the lowest. No clear reason is apparent for this difference. The dominance of short-chain PFAS in the bivalves is consistent with their predominant relative contribution in water (i.e., PFBA and PFBS) and sediment (i.e., PFBA and FBSA). Even though short-chain PFAS are not generally considered bioaccumulative (Brendel et al., 2018), their detection in the bivalves of this study likely reflects the continuous exposure from water and sediment.

SS and NTA of bivalves detected 9 PFAS compounds at different CLs (Fig. S3; Table S6), with all compounds semi-quantified except for  $C_{13}H_{11}F_{17}OS$  and  $C_{13}H_{2}F_{24}O_{5}N$  (Table S7). The estimated concentrations revealed that TFCPrA was the predominant PFAS of those detected

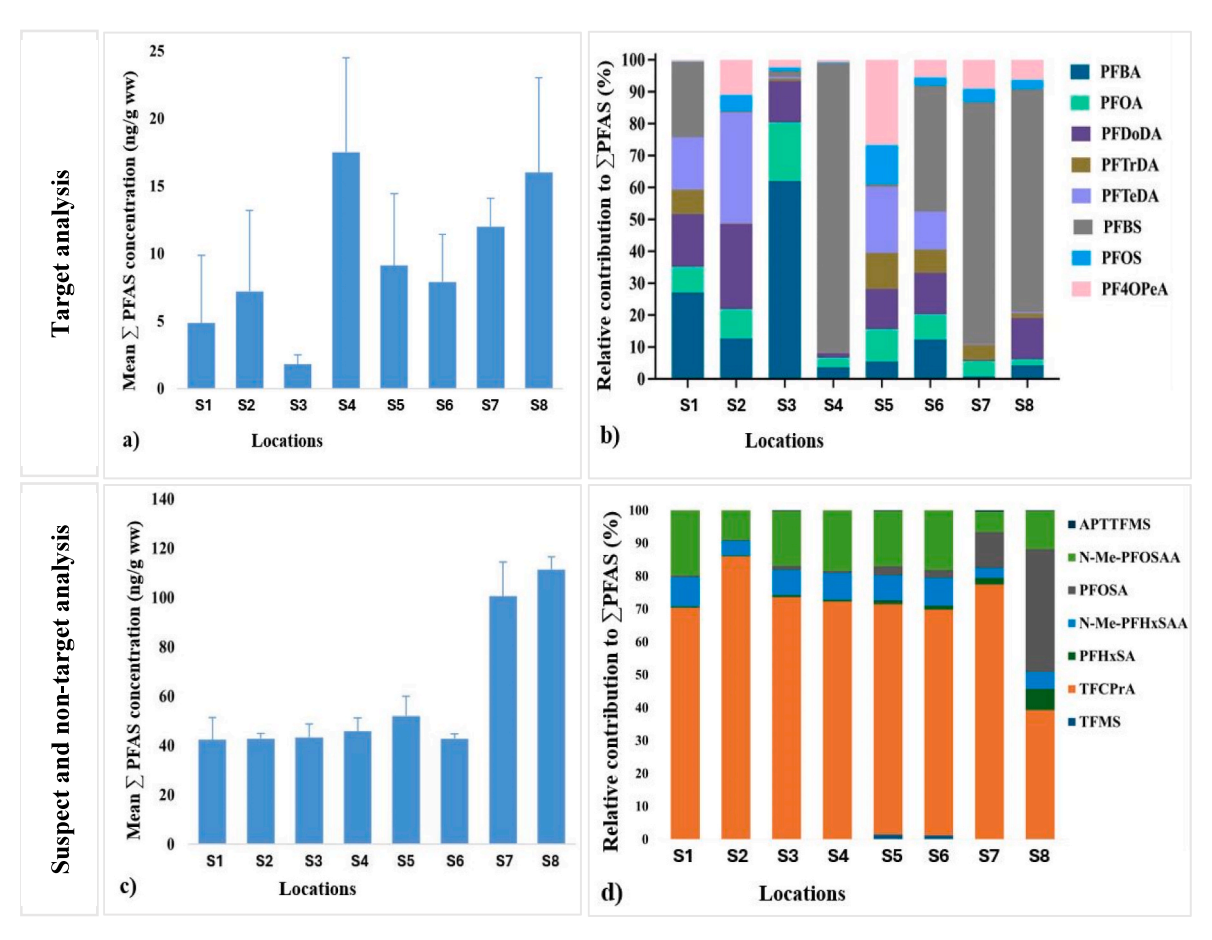


Fig. 4. a) Mean  $\sum$ PFAS concentrations accumulated in bivalves (ng/g ww; n = 5); b) molar-based relative contribution of individual PFAS to the  $\sum$ PFAS concentration by target analysis; c) mean estimated  $\sum$ PFAS concentrations through semi-quantification (ng/g ww; n = 5); and d) molar-based relative contribution of individual PFAS to the estimated  $\sum$ PFAS concentration profile (100 %) at each location investigated by suspect screening and non-target analysis.

with SS and NTA at all locations except at S8, where PFOSA had a higher estimated concentration of 65  $\pm$  8 ng/g ww (Table S7). The highest estimated average TFCPrA concentration was observed at S7 (58  $\pm$  44 ng/g ww), and it was a significant contributor to the  $\sum$ PFAS concentration at all locations (Fig. 4d). Furthermore, average estimated  $\sum$ PFAS concentrations showed an increasing trend downstream along the estuary, with the lowest concentration at the most upstream location, S1 (42  $\pm$  8.9 ng/g ww), and the highest at the downstream location, S8 (111  $\pm$  5 ng/g ww) (Fig. 4c).

Similar to water and sediment, ultra-short-chain (TFMS), short-chain (TFCPrA), and long-chain PFAS were detected in bivalves with SS and NTA. However, unlike in water and sediment, TFMS was infrequently detected in bivalves, suggesting that bivalves do not readily accumulate TFMS. Instead, TFCPrA had a high detection frequency and high concentrations at most locations, also dominating the  $\sum$ PFAS concentrations accumulated in bivalves. To the best of our knowledge, this is the first study to report the detection of TFCPrA in biota samples. In addition, the environmental occurrence and sources of TFCPrA are unclear.

#### 3.4. Relationship of PFAS in bivalves with the abiotic environment

Comparing the accumulated PFAS profiles in bivalves with the abiotic samples, PFBA, PFOS, PFOA, PF4OPeA, and PFTrDA were detected in both water and sediment, indicating uptake in bivalves from the abiotic environment. However, PFTeDA was detected in bivalves, while it was <LOQ in both water and sediment. It might be present in the abiotic environment in low concentrations and accumulated to quantifiable levels in bivalves over time. The compound PFDoDA was detected in sediment but not in water, while PFBS was found in water but not in sediment, with its presence varying by location. In contrast, despite being present in both sediment and water, 6:2 FTS was not detected in bivalves, likely due to its transformation in the environment. This was consistent with a previous study suggesting a lower likelihood of bioaccumulation of this compound in aquatic organisms (Hoke et al., 2015). In addition, among the PFAS detected in bivalves through SS and NTA, TFMS, N-Me-PFHxSAA, PFOSA, TFCPrA, and N-Me-PFOSAA were

identified both in water and sediment. However, APTTFMS and PFHxSA were only detected in water and sediment, respectively, explaining their occurrence in bivalves.

The relationships between PFAS accumulated in bivalves and the abiotic environment along with water and sediment characteristics are summarized in Tables S8-S10. Multivariate analysis of \( \sumset \text{PFAS con-} centrations across different matrices investigated by target analysis (Fig. 5a; Table S11) showed a negative correlation between the  $\Sigma$ PFAS concentrations accumulated in bivalves (PFAS<sub>bivalves</sub>) and those in sediment (PFAS<sub>sediment</sub>) (r = -0.71, p = 0.0003; Table S9), while no correlation was found with ∑PFAS concentrations in water (PFAS<sub>water</sub>) (r = 0.08, p = 0.72; Table S8). Similarly, estimated  $\Sigma$ PFAS concentrations in bivalves showed negative correlations with concentrations in sediment (r = -0.5, p = 0.01), while no correlation was observed with water concentrations (r =-0.3, p =0.14). A significant positive correlation of PFAS $_{\text{sediment}}$  with both TOC and clay content was shown also by the PCA biplot (p < 0.05; Table S9). The positive correlation of PFASwater and pH was indicated by the PCA; however, it was not statistically significant (p > 0.5; Table S8). Similar to the results of the PCA, multiple regression analysis revealed that PFAS in bivalves showed a negative relationship with  $PFAS_{sediment}$ , while no associations were found with PFAS<sub>water</sub> and water-sediment characteristics (PFAS<sub>bivalves</sub> = 17.4–0.2 PFAS<sub>sediment</sub>,  $R^2 = 0.36$ ).

The inverse relationship of ∑PFAS concentrations in bivalves and sediments suggests that the sorption of PFAS to sediment reduces their bioavailability to bivalves. This may be influenced by the exposure in cages, as the Asian clams were exposed to the upper water column without being in contact with the sediment at Sea Scheldt locations. In addition, TOC and clay content may enhance PFAS retention in sediments while reducing their bioavailability, as shown by significant positive correlations between PFAS concentrations in sediment with both TOC and clay content. Furthermore, salinity might affect the partitioning of certain PFAS in estuaries by different mechanisms, although the dominant mechanism may vary depending on the characteristics of the sorbent (e.g., organic versus mineral composition) and the chemical properties of the PFAS (e.g., chain length, functional group, and charge

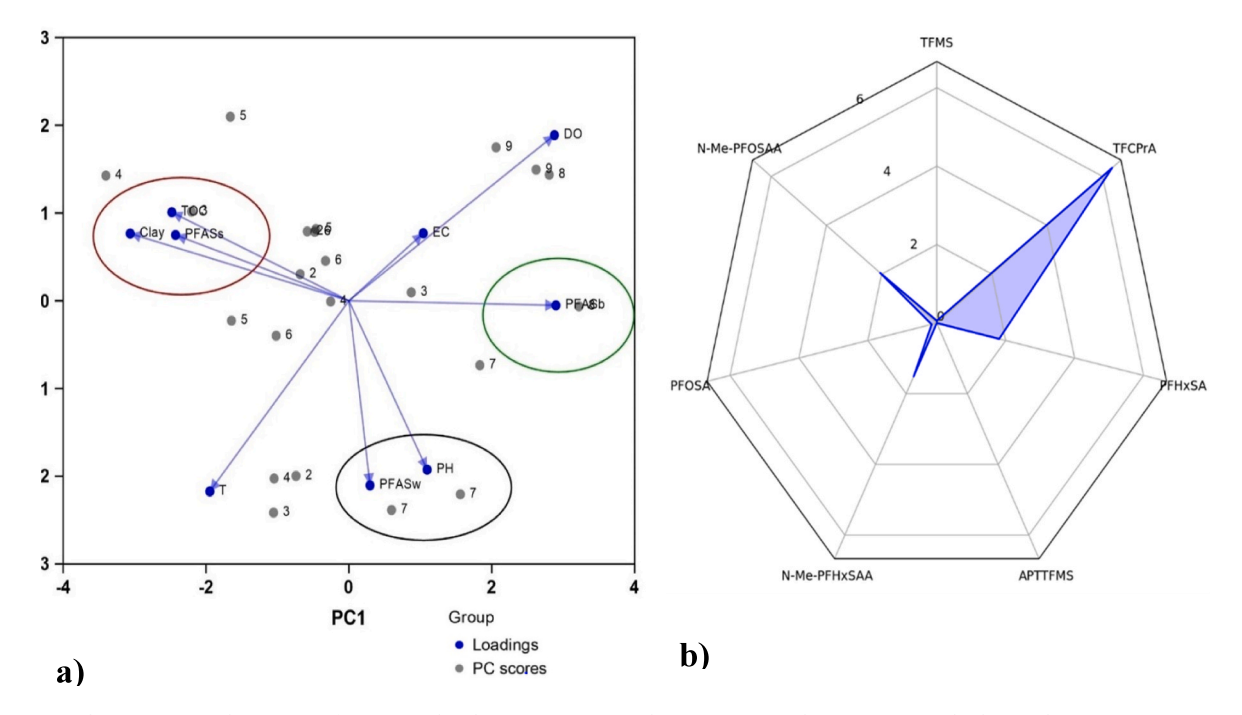


Fig. 5. a) Principal Component Analysis (PCA) of  $\sum$ PFAS in bivalves (PFAS<sub>b</sub>; green color),  $\sum$ PFAS in sediment (PFAS<sub>b</sub>; red color), and  $\sum$ PFAS in water (PFAS<sub>w</sub>; black color), along with pH, conductivity (EC), clay content (C), and Total organic carbon (TOC) content summarized in Table S11; b) Spider plot for biota sediment accumulation factor indicating the accumulation from sediment to bivalves for individual PFAS compounds identified via suspect and non-target analysis. (For interpretation of the references to color in this figure legend, the reader is referred to the Web version of this article.)

characteristics) (Cai et al., 2022; Li et al., 2022). These mechanisms include salting-out effects that reduce PFAS solubility in water, cation bridging between anionic PFAS functional groups and negatively charged sediment surfaces, and the reduction of electrostatic repulsion both among PFAS molecules and between PFAS and sorbent surfaces. Additionally, increased hydrophobic interactions between PFAS alkyl chains and organic matter in the sediment further promote retention. These mechanisms enhance adsorption to sediment and, consequently, reduce their bioavailability to pelagic organisms (Li et al., 2022). A positive correlation between PFAS concentrations in water and bivalves was expected; however, this was not observed and might be explained by different factors. The dynamic nature of estuarine environments, such as changes in salinity, water flow, and physical disturbances caused by tidal actions, influences both PFAS distribution and bioavailability, potentially affecting the correlation.

In addition to investigating \( \sumeter PFAS \) concentrations using PCA exploration and logistic regression, BAF<sub>Bivalves; Scheldt Estuary</sub> and BSAF-Bivalves; Scheldt Estuary were used to assess the uptake of individual PFAS compounds from the abiotic environment (Table S10), TFMS, PFBA, and PFOSA showed no bioaccumulation potential from sediment at any location (BSAF  $_{\mbox{\footnotesize Bivalves; Scheldt Estuary}} < 1;$  Table S10). In contrast, PF4O-PeA, TFCPrA, N-Me-PFOSAA, and PFTrDA demonstrated bioaccumulation potential from sediment at most sites investigated (at least at 6 out of 8; BSAF<sub>Bivalves</sub>; <sub>Scheldt Estuary</sub> > 1) (Table S10). Although PFAS are retained in sediment, disturbances in estuarine ecosystems, such as tides and waves, can resuspend sediments, potentially releasing PFAS and enhancing their bioavailability (Anik et al., 2025). Among these, TFCPrA had the highest BSAF<sub>Bivalves: Scheldt Estuary</sub>, ranging from 2.9 at S6 to 16.4 at S7 (Fig. 5b). However, BSAF values should be interpreted with caution, as clams in this study were exposed to the water column without direct contact with the sediment bed at most locations. Although these exposure conditions may not be ideal for determining BSAF values, observations of BSAF values > 1 suggest that PFAS bound to sediments may become resuspended and subsequently accumulate in clams. Concerning BAF<sub>Bivalves; Scheldt Estuary</sub>, PFAS such as PFBS (except at S7), TFCPrA, N-Me-PFHxSAA, and PFOSA had BAFBivalves; Scheldt Estuary values > 1, indicating an accumulation potential from water and dietary sources present in the water (Table S10). On the other hand, BAF<sub>Bivalves</sub>; Scheldt Estuary < 1 was found for PFOA and APTTFMS (Table S10), although PFOA is a bioaccumulative compound according to the United Nations Stockholm Convention on Persistent Organic Pollutants (UNEP, 2019).

### 4. Conclusions

Both legacy and emerging PFAS were detected in water, sediment, and bivalves of the Scheldt estuary, with varying concentrations and profiles. A notable dominance of short-chain PFAS concentrations in both the abiotic environment and bivalves was detected, likely reflecting the production shift from long-chain to short-chain alternatives with resulting environmental emissions and distribution. Their detection in bivalves is noteworthy and challenges the general assumption that short-chain PFAS do not accumulate in biota. It remains to be shown whether this is a feature specific to bivalves or whether this observation is mainly related to the continuous exposure through contaminated water and particles in this study. These findings support the integration of bivalve biomonitoring into routine environmental assessments of PFAS pollution. Additionally, the ultra-short chain TFMS was detected at exceptionally high estimated concentrations in water near industrial areas. This presence and dominance of the short-chain PFAS highlights the need for further information for risk assessments and potential regulatory action. While this study provides valuable insights into the distribution of PFAS in estuarine ecosystems, it also shows a highly complex and dynamic combination of factors potentially influencing PFAS fate and transport in this environment. Future research should broaden the scope by incorporating the tidal cycle in sampling and

including SPM to better understand the fate of PFAS in estuarine environments and associated exposure risks. Sampling campaigns should integrate SPM collection using instruments such as sedimentation traps to provide insights into particulate-associated PFAS occurrence and their role in bioavailability.

#### CRediT authorship contribution statement

Musa Bonso: Writing – original draft, Visualization, Methodology, Investigation, Formal analysis, Data curation, Conceptualization. Francesca Cappelli: Writing – review & editing, Validation, Methodology, Funding acquisition, Formal analysis. Fabian Simon: Writing – review & editing, Validation, Methodology, Formal analysis. Katrin Vorkamp: Writing – review & editing, Project administration, Funding acquisition, Conceptualization. Laetitia Six: Writing – review & editing, Project administration, Funding acquisition, Conceptualization. Georgios Niarchos: Writing – review & editing, Project administration, Funding acquisition, Conceptualization. Adrian Covaci: Writing – review & editing, Validation, Methodology, Funding acquisition, Formal analysis. Lieven Bervoets: Writing – review & editing, Supervision, Methodology, Funding acquisition, Conceptualization. Thimo Groffen: Writing – review & editing, Supervision, Methodology, Funding acquisition, Conceptualization.

## **Funding**

This work was funded by the Vlaamse Interuniversitaire Raad - University Development Cooperation (VLIR-UOS) through a scholarship grant awarded to MB and by the Research Foundation Flanders through a senior postdoctoral research grant to TG (grant number 1205724N). FC acknowledges a post-doctoral fellowship from the European Partnership for the Assessment of Risks from Chemicals (PARC). FS acknowledges the University of Antwerp for the post-doctoral fellowship under the Post-doc Challenge (Antigoon number 48295). This work was carried out in the framework of the PARC and has received funding from the European Union's Horizon Europe research and innovation programme under Grant Agreement No 101057014. Views and opinions expressed are, however, those of the author(s) only and do not necessarily reflect those of the European Union or the Health and Digital Executive Agency. Neither the European Union nor the granting authority can be held responsible for them.

### **Declaration of competing interest**

The authors declare that they have no known competing financial interests or personal relationships that could have appeared to influence the work reported in this paper.

## Acknowledgements

The authors would also like to thank the Vlaamse Waterweg for giving permission of exposing the clams to the pontoons of the waterbus, and Tim Willems for the target analysis.

### Appendix A. Supplementary data

Supplementary data to this article can be found online at  $\frac{https:}{doi.}$  org/10.1016/j.envpol.2025.127349.

## Data availability

Data will be made available on request.

#### References

- 3M Company, 2022. 1st gefaseerd beschrijvend bodemonderzoek. Available from: http s://multimedia.3m.com/mws/media/2226394O/dsi-report-by-erm-2022.pdf. (Accessed 3 June 2025).
- Ahrens, L., Bundschuh, M., 2014. Fate and effects of poly- and perfluoroalkyl substances in the aquatic environment: a review. Environ. Toxicol. Chem. 33 (9), 1921–1929. https://doi.org/10.1002/etc.2663.
- Anik, A.H., Basir, M.S., Sultan, M.B., Alam, M., Rahman, M.M., Tareq, S.M., 2025. Unveiling the emerging concern of per- and polyfluoroalkyl substances (PFAS) and their potential impacts on estuarine ecosystems. Mar. Pollut. Bull. 212, 117554. https://doi.org/10.1016/j.marpolbul.2025.117554.
- Arnot, J.A., Gobas, F.A.P.C., 2006. A review of bioconcentration factor (BCF) and bioaccumulation factor (BAF) assessments for organic chemicals in aquatic organisms. Environ. Rev. 14 (4), 257–297. https://doi.org/10.1139/A06-005.
- Bervoets, L., Voets, J., Chu, S., Covaci, A., Schepens, P., Blust, R., 2004. Comparison of accumulation of micropollutants between indigenous and transplanted zebra mussels (*Dreissena polymorpha*). Environ. Toxicol. Chem. 23 (8), 1973–1983. https://doi.org/10.1897/03-365.
- Bervoets, L., Voets, J., Smolders, R., Blust, R., 2005. Metal accumulation and condition of transplanted zebra mussel (*Dreissena polymorpha*) in metal polluted rivers. Aquat. Ecosys. Health Manag. 8 (4), 451–460. https://doi.org/10.1080/ 14634980500360100.
- Beyer, J., Green, N.W., Brooks, S., Allan, I.J., Ruus, A., Gomes, T., Bråte, I.L.N., Schøyen, M., 2017. Blue mussels (*Mytilus edulis* spp.) as sentinel organisms in coastal pollution monitoring: a review. Mar. Environ. Res. 130, 338–365. https://doi.org/ 10.1016/j.marenyres.2017.07.024.
- Björnsdotter, M.K., Yeung, L.W.Y., Kärrman, A., Jogsten, I.E., 2019. Ultra-short-chain perfluoroalkyl acids including trifluoromethane sulfonic acid in water connected to known and suspected point sources in Sweden. Environ. Sci. Technol. 53 (19), 11093–11101. https://doi.org/10.1021/acs.est.9b02211.
- Bonso, M., Bervoets, L., Flipkens, G., Groffen, T., 2025. Accumulation of metals in resident blue mussels (*Mytilus edulis*) and exposed Asian clams (*Corbicula fluminea*) along the Scheldt Estuary: a spatial and temporal investigation. Mar. Pollut. Bull. 213, 117619. https://doi.org/10.1016/j.marpolbul.2025.117619.
- Bråte, I.L.N., Hurley, R., Iversen, K., Beyer, J., Thomas, K.V., Steindal, C.C., Green, N.W., Olsen, M., Lusher, A., 2018. Mytilus spp. as sentinels for monitoring microplastic pollution in Norwegian coastal waters: a qualitative and quantitative study. Environ. Pollut. 243, 383–393. https://doi.org/10.1016/j.envpol.2018.08.077.
- Brendel, S., Fetter, É., Staude, C., Vierke, L., Biegel-Engler, A., 2018. Short-chain perfluoroalkyl acids: environmental concerns and a regulatory strategy under REACH. Environ. Sci. Eur. 30 (1), 9. https://doi.org/10.1186/s12302-018-0134-4.
- Buck, R.C., Franklin, J., Berger, U., Conder, J.M., Cousins, I.T., Voogt, P. De, Jensen, A. A., Kannan, K., Mabury, S.A., van Leeuwen, S.P.J., 2011. Perfluoroalkyl and polyfluoroalkyl substances in the environment: terminology, classification, and origins. Integrated Environ. Assess. Manag. 7 (4), 513–541. https://doi.org/10.1002/jeam.258.
- Byns, C., Teunen, L., Groffen, T., Lasters, R., Bervoets, L., 2022. Bioaccumulation and trophic transfer of perfluorinated alkyl substances (PFAS) in marine biota from the Belgian North Sea: distribution and human health risk implications. Environ. Pollut. 311, 119907. https://doi.org/10.1016/j.envpol.2022.119907.
- Byns, C., Groffen, T., Bervoets, L., 2024. Aquatic macroinvertebrate community responses to pollution of perfluoroalkyl substances (PFAS): can we define threshold body burdens? Sci. Total Environ. 917, 170611. https://doi.org/10.1016/j. scitotenv.2024.170611.
- Cai, W., Navarro, D.A., Du, J., Ying, G., Yang, B., McLaughlin, M.J., Kookana, R.S., 2022. Increasing ionic strength and valency of cations enhance sorption through hydrophobic interactions of PFAS with soil surfaces. Sci. Total Environ. 817. https:// doi.org/10.1016/j.scitotenv.2022.152975.
- Cappelli, F., Ait Bamai, Y., Van Hoey, K., Kim, D.-H., Covaci, A., 2024. Occurrence of short- and ultra-short chain PFAS in drinking water from Flanders (Belgium) and implications for human exposure. Environ. Res. 260, 119753. https://doi.org/ 10.1016/j.envres.2024.119753.
- Charbonnet, J.A., McDonough, C.A., Xiao, F., Schwichtenberg, T., Cao, D., Kaserzon, S., Thomas, K.V., Dewapriya, P., Place, B.J., Schymanski, E.L., Field, J.A., Helbling, D. E., Higgins, C.P., 2022. Communicating confidence of Per- and Polyfluorolkyl substance identification via high-resolution mass spectrometry. Environ. Sci. Technol. Lett. 9 (6), 473–481. https://doi.org/10.1021/acs.estlett.2c00206.
- Chu, S., Letcher, R.J., McGoldrick, D.J., Backus, S.M., 2016. A new fluorinated surfactant contaminant in Biota: perfluorobutane sulfonamide in several fish species. Environ. Sci. Technol. 50 (2), 669–675. https://doi.org/10.1021/acs.est.5b05058.
- D'Hollander, W., De Bruyn, L., Hagenaars, A., de Voogt, P., Bervoets, L., 2014. Characterization of perfluorooctane sulfonate (PFOS) in a terrestrial ecosystem near a fluorochemical plant in Flanders, Belgium. Environ. Sci. Pollut. Control Ser. 21 (20), 11856–11866. https://doi.org/10.1007/s11356-013-2449-4.
- European Union (EU), 2013. Directives of 12 August 2013 amending directives 2000/60/EC and 2008/105/EC as regards priority substances in the field of water policy. Off. J. Eur. Union L226, 1–17.
- Flemish environmental agency, 2018. Annex 2.3.1. basic environmental quality standards for surface water. https://navigator.emis.vito.be/detail?woId=10071.
- Gaines, L.G.T., 2023. Historical and current usage of per- and polyfluoroalkyl substances (PFAS): a literature review. Am. J. Ind. Med. 66 (5), 353–378. https://doi.org/10.1002/ajim.23362.
- Gao, G., O'Sullivan, J.J., Corkery, A., Bedri, Z., O'Hare, G.M.P., Meijer, W.G., 2023. The use of transport time scales as indicators of pollution persistence in a macro-tidal setting. J. Mar. Sci. Eng. 11 (5), 1073. https://doi.org/10.3390/jmse11051073.

- Glüge, J., Scheringer, M., Cousins, I.T., Dewitt, J.C., Goldenman, G., Herzke, D., Lohmann, R., Ng, C.A., Trier, X., Wang, Z., 2020. An overview of the uses of per- and polyfluoroalkyl substances (PFAS). Environ. Sci.: Process. Impacts 22 (12), 2345–2373. https://doi.org/10.1039/d0em00291g.
- Groffen, T., Eens, M., Bervoets, L., 2019a. Do concentrations of perfluoroalkylated acids (PFAAs) in isopods reflect concentrations in soil and songbirds? A study using a distance gradient from a fluorochemical plant. Sci. Total Environ. 657, 111–123. https://doi.org/10.1016/J.SCITOTENV.2018.12.072.
- Groffen, T., Lasters, R., Lopez-Antia, A., Prinsen, E., Bervoets, L., Eens, M., 2019b. Limited reproductive impairment in a passerine bird species exposed along a perfluoroalkyl acid (PFAA) pollution gradient. Sci. Total Environ. 652, 718–728. https://doi.org/10.1016/j.scitotenv.2018.10.273.
- Groffen, T., Lasters, R., Lemière, F., Willems, T., Eens, M., Bervoets, L., Prinsen, E., 2019c. Development and validation of an extraction method for the analysis of perfluoroalkyl substances (PFASs) in environmental and biotic matrices.
  J. Chromatogr. B 1116, 30–37. https://doi.org/10.1016/j.jchromb.2019.03.034.
- Groffen, T., Bervoets, L., Eens, M., 2023. Temporal trends in PFAS concentrations in livers of a terrestrial raptor (common buzzard; *Buteo buteo*) collected in Belgium during the period 2000–2005 and in 2021. Environ. Res. 216, 114644. https://doi. org/10.1016/j.envres.2022.114644.
- Groffen, T., Keirsebelik, H., Dendievel, H., Falcou-Préfol, M., Bervoets, L., Schoelynck, J., 2024. Are Chinese mitten crabs (*Eriocheir sinensis*) suitable as biomonitor or bioindicator of per- and polyfluoroalkyl substances (PFAS) pollution? J. Hazard Mater. 464, 133024. https://doi.org/10.1016/j.jhazmat.2023.133024.
- Guo, M., Zheng, G., Peng, J., Meng, D., Wu, H., Tan, Z., Li, F., Zhai, Y., 2019. Distribution of perfluorinated alkyl substances in marine shellfish along the Chinese Bohai Sea Coast. J. Environ. Sci. Health - Part B Pesticides, Food Contam. Agric. Wastes 54 (4), 271–280. https://doi.org/10.1080/03601234.2018.1559570.
- Guo, M., Wu, F., Geng, Q., Wu, H., Song, Z., Zheng, G., Peng, J., Zhao, X., Tan, Z., 2023. Perfluoroalkyl substances (PFASs) in aquatic products from the Yellow-Bohai Sea coasts, China: concentrations and profiles across species and regions. Environ. Pollut. 327, 121514. https://doi.org/10.1016/j.envpol.2023.121514.
- Heiri, O., Lotter, A.F., Lemcke, G., 2001. Loss on ignition as a method for estimating organic and carbonate content in sediments: reproducibility and comparability of results. J. Paleolimnol. 25 (1), 101–110. https://doi.org/10.1023/A: 1008119611481.
- Hoke, R.A., Ferrell, B.D., Ryan, T., Sloman, T.L., Green, J.W., Nabb, D.L., Mingoia, R., Buck, R.C., Korzeniowski, S.H., 2015. Aquatic hazard, bioaccumulation and screening risk assessment for 6:2 fluorotelomer sulfonate. Chemosphere 128, 258–265. https://doi.org/10.1016/j.chemosphere.2015.01.033.
- Hollender, J., Schymanski, E.L., Ahrens, L., Alygizakis, N., Béen, F., Bijlsma, L., Brunner, A.M., Celma, A., Fildier, A., Fu, Q., Gago-Ferrero, P., Gil-Solsona, R., Haglund, P., Hansen, M., Kaserzon, S., Kruve, A., Lamoree, M., Margoum, C., Meijer, J., et al., 2023. NORMAN guidance on suspect and non-target screening in environmental monitoring. Environ. Sci. Eur. 35 (1), 75. https://doi.org/10.1186/s12302-023-00779-4.
- ITRC, 2023. Per- and polyfluoroalkyl substances (PFAS) technical and regulatory guidance document. In: Emerging Contaminants Handbook. Interstate Technology & Regulatory Council. December, 1-534. https://pfas-1.itrcweb.org/wp-content/uploads/2023/12/Full-PFAS-Guidance-12.11.2023.pdf.
- Jeon, J., Kannan, K., Lim, H.K., Moon, H.B., Ra, J.S., Kim, S., 2010. Bioaccumulation of perfluorochemicals in pacific oyster under different salinity gradients. Environ. Sci. Technol. 44 (7), 2695–2701. https://doi.org/10.1021/es100151r.
  Koban, L.A., King, T., Huff, T.B., Furst, K.E., Nelson, T.R., Pfluger, A.R., Kuppa, M.M.,
- Koban, L.A., King, T., Hutf, T.B., Furst, K.E., Nelson, T.R., Pfluger, A.R., Kuppa, M.M., Fowler, A.E., 2024. Passive biomonitoring for per- and polyfluoroalkyl substances using invasive clams, C. fluminea. J. Hazard Mater. 472, 134463. https://doi.org/ 10.1016/j.jhazmat.2024.134463.
- Kurwadkar, S., Dane, J., Kanel, S.R., Nadagouda, M.N., Cawdrey, R.W., Ambade, B., Struckhoff, G.C., Wilkin, R., 2022. Per- and polyfluoroalkyl substances in water and wastewater: a critical review of their global occurrence and distribution. Sci. Total Environ. 809, 151003. https://doi.org/10.1016/j.scitotenv.2021.151003.
- Lauria, M.Z., Sepman, H., Ledbetter, T., Plassmann, M., Roos, A.M., Simon, M., Benskin, J.P., Kruve, A., 2024. Closing the organofluorine mass balance in marine mammals using suspect screening and machine learning-based quantification. Environ. Sci. Technol. 58 (5), 2458–2467. https://doi.org/10.1021/acs.est.3c07220.
- Lenka, S.P., Kah, M., Padhye, L.P., 2022. Occurrence and fate of poly- and perfluoroalkyl substances (PFAS) in urban waters of New Zealand. J. Hazard Mater. 428, 128257. https://doi.org/10.1016/j.jhazmat.2022.128257.
- Li, C., Zhang, C., Gibbes, B., Wang, T., Lockington, D., 2022. Coupling effects of tide and salting-out on perfluorooctane sulfonate (PFOS) transport and adsorption in a coastal aquifer. Adv. Water Resour. 166, 104240. https://doi.org/10.1016/j. advwatres 2022 104240
- Liu, Y., D'Agostino, L.A., Qu, G., Jiang, G., Martin, J.W., 2019. High-resolution mass spectrometry (HRMS) methods for nontarget discovery and characterization of polyand per-fluoroalkyl substances (PFASs) in environmental and human samples. Trends Anal. Chem. 121, 115420. https://doi.org/10.1016/j.trac.2019.02.021.
- Liu, C., Ma, X.X., Wang, S.Q., Li, Q., Cheng, P., Hou, W., Li, Y.Y., Li, W.L., Wang, X.H., 2024. Fractionation and tidal characteristics of per- and polyfluoroalkyl substances in the estuarine maximum turbidity zone. Sci. Total Environ. 20, 957. https://doi. org/10.1016/j.scitotenv.2024.177646.
- Lopez-Antia, A., Groffen, T., Lasters, R., Abdelgawad, H., Sun, J., Asard, H., Bervoets, L., Eens, M., 2019. Perfluoroalkyl acids (PFAAs) concentrations and oxidative status in two generations of great tits inhabiting a contamination hotspot. Environ. Sci. Technol. 53 (3), 1617–1626. https://doi.org/10.1021/acs.est.8b05235.
- Manz, K.E., Feerick, A., Braun, J.M., Feng, Y.L., Hall, A., Koelmel, J., Manzano, C., Newton, S.R., Pennell, K.D., Place, B.J., Godri Pollitt, K.J., Prasse, C., Young, J.A.,

- 2023. Non-targeted analysis (NTA) and suspect screening analysis (SSA): a review of examining the chemical exposome. J. Expo. Sci. Environ. Epidemiol. 33 (4), 524–536. https://doi.org/10.1038/s41370-023-00574-6.
- McLusky, D.S., Elliott, M., 2010. The estuarine ecosystem. In: The Estuarine Ecosystem. Oxford University Press. https://doi.org/10.1093/acprof:oso/ 9780198525080.001.0001.
- McMahon, R.F., 2002. Evolutionary and physiological adaptations of aquatic invasive animals: r selection versus resistance. Can. J. Fish. Aquat. Sci. 59 (7), 1235–1244. https://doi.org/10.1139/f02-105.
- Meire, P., Ysebaert, T., Van Damme, S., Van Den Bergh, E., Maris, T., Struyf, E., 2005. The Scheldt Estuary: a description of a changing ecosystem. Hydrobiologia 540 (1–3). https://doi.org/10.1007/s10750-005-0896-8.
- Mijangos, L., Žiarrusta, H., Ros, O., Kortazar, L., Fernández, L.A., Olivares, M., Zuloaga, O., Prieto, A., Etxebarria, N., 2018. Occurrence of emerging pollutants in estuaries of the Basque Country: analysis of sources and distribution, and assessment of the environmental risk. Water Res. 147, 152–163. https://doi.org/10.1016/j. watres 2018.09.033
- Moriwaki, H., Tian, Y.S., Kawashita, N., Takagi, T., 2018. Mordred: a molecular descriptor calculator. J. Cheminf. 10 (1). https://doi.org/10.1186/s13321-018
- Mu, H., Yang, Z., Chen, L., Gu, C., Ren, H., Wu, B., 2024. Suspect and nontarget screening of per- and polyfluoroalkyl substances based on ion mobility mass spectrometry and machine learning techniques. J. Hazard Mater. 461, 132669. https://doi.org/ 10.1016/j.jbazmat.2023.132669.
- OECD, 2021. Reconciling terminology of the universe of Per- and polyfluoroalkyl substances: recommendations and practical guidance. OECD Series on Risk Management No.61. https://one.oecd.org/document/ENV/CBC/MONO(2021) 25/Fn/ndf.
- Plancke, Y., Maris, T., Verleye, T., Sandra, M., 2023. Scheldt Estuary. Compendium Voor Kust En Zee = Compendium for Coast and Sea, vol 2023, pp. 1–12. https://doi.org/ 10.48470/60
- Podder, A., Sadmani, A.H.M.A., Reinhart, D., Chang, N. Bin, Goel, R., 2021. Per and poly-fluoroalkyl substances (PFAS) as a contaminant of emerging concern in surface water: a transboundary review of their occurrences and toxicity effects. J. Hazard Mater. 419, 126361. https://doi.org/10.1016/j.jhazmat.2021.126361.
- Powley, C.R., George, S.W., Ryan, T.W., Buck, R.C., 2005. Matrix effect-free analytical methods for determination of perfluorinated carboxylic acids in environmental matrixes. Anal. Chem. 77 (19), 6353–6358. https://doi.org/10.1021/ac0508090.
- Rehman, A.U., Crimi, M., Andreescu, S., 2023. Current and emerging analytical techniques for the determination of PFAS in environmental samples. Trend. Environ. Anal. Chem. 37, e00198. https://doi.org/10.1016/j.teac.2023.e00198.
- Schlabach, M., Haglund, P., Reid, M., Rostkowski, P., 2017. Suspect Screening in Nordic Countries. Nordic Council of Ministers. https://doi.org/10.6027/TN2017-561.
- Schulze, S., Zahn, D., Montes, R., Rodil, R., Quintana, J.B., Knepper, T.P., Reemtsma, T., Berger, U., 2019. Occurrence of emerging persistent and mobile organic contaminants in European water samples. Water Res. 153, 80–90. https://doi.org/ 10.1016/j.watres.2019.01.008.
- Schymanski, E.L., Zhang, J., Thiessen, P.A., Chirsir, P., Kondic, T., Bolton, E.E., 2023.

  Per- and polyfluoroalkyl substances (PFAS) in PubChem: 7 million and growing.

- Environ. Sci. Technol. 57 (44), 16918–16928. https://doi.org/10.1021/acs.est 3c04855
- Sultan, M.B., Anik, A.H., Rahman, Md M., 2024. Emerging contaminants and their potential impacts on estuarine ecosystems: are we aware of it? Mar. Pollut. Bull. 199, 115982. https://doi.org/10.1016/j.marpolbul.2023.115982.
- Teunen, L., Bervoets, L., Belpaire, C., De Jonge, M., Groffen, T., 2021. PFAS accumulation in indigenous and translocated aquatic organisms from Belgium, with translation to human and ecological health risk. Environ. Sci. Eur. 33 (1), 39. https://doi.org/10.1186/s12302-021-00477-z.
- Trier, X., Van-Leeuwen, S.P.J., Brambilla, G., Weber, R., Webster, T.F., 2025. The critical role of commercial analytical reference standards in the control of chemical risks: the case of PFAS and ways forward. Environ. Health Perspect. 133 (1), 15001. https:// doi.org/10.1289/EHP12331.
- United Nations Environment Programme, 2019. Stockholm convention on persistent organic pollutants (POPs). Ninth Meeting of the Conference of the Parties (COP-9). Geneva, Switzerland, 29 April–10 May 2019. https://www.pops.int/TheConvention/ConferenceoftheParties/Meetings/COP9/tabid/7521/Default.aspx.
- Van Ael, E., Covaci, A., Blust, R., Bervoets, L., 2012. Persistent organic pollutants in the Scheldt Estuary: environmental distribution and bioaccumulation. Environ. Int. 48, 17–27. https://doi.org/10.1016/j.envint.2012.06.017.
- Van Ael, E., Blust, R., Bervoets, L., 2017. Metals in the Scheldt Estuary: from environmental concentrations to bioaccumulation. Environ. Pollut. 228, 82–91. https://doi.org/10.1016/j.envpol.2017.05.028.
- Villanueva, P., 2005. MLE-Based Procedure for left-censored Data Excel Spreadsheet. U. S. Environmental protection Agency, Washington D.C.. Office of Pesticide Programs.
- VRT.be, 2021. Chemiebedrijf 3M geeft nu zelf aan dat het de mogelijk giftige stof FBSA in de Schelde loost HLN. Retrieved March 12, 2025, from. https://www.vrt.be/vrtnws/nl/2021/08/24/chemiebedrijf-3m-geeft-nu-zelf-aan-dat-het-giftige-stof-fbsa-in/.
- Waterschap Scheldestromen, 2024. Resultaten onderzoeksrapport PFAS 2024. https://scheldestromen.nl/resultaten-onderzoeks-rapport-pfas-2024.
- Yan, P.-F., Dong, S., Woodcock, M.J., Manz, K.E., Garza-Rubalcava, U., Abriola, L.M., Pennell, K.D., Cápiro, N.L., 2024. Biotransformation of 6:2 fluorotelomer sulfonate and microbial community dynamics in water-saturated one-dimensional flowthrough columns. Water Res. 252, 121146. https://doi.org/10.1016/j. watres.2024.121146.
- Zhang, Y., Li, J., Yan, N., Alshebel, B.H., Brusseau, M.L., 2025. Contrasting adsorption behavior of perfluorooctane sulfonic acid and its precursor perfluorooctane sulfonamide characterized by bench-scale-corroborated density-functional-theory analysis. J. Hydrol. 659, 133274. https://doi.org/10.1016/j.jhydrol.2025.133274.
- Zhong, H., Zheng, M., Liang, Y., Wang, Y., Gao, W., Wang, Y., Jiang, G., 2021. Legacy and emerging per- and polyfluoroalkyl substances (PFAS) in sediments from the East China Sea and the Yellow Sea: occurrence, source apportionment and environmental risk assessment. Chemosphere 282, 131042. https://doi.org/10.1016/j.chemosphere.2021.131042.
- Zweigle, J., Bugsel, B., Fabregat-Palau, J., Zwiener, C., 2024. PFΔScreen an open-source tool for automated PFAS feature prioritization in non-target HRMS data. Anal. Bioanal. Chem. 416 (2), 349–362. https://doi.org/10.1007/s00216-023-05070.2